International Journal of Nanomedicine

Dovepress
Taylor & Francis Group

Open Access Full Text Article

ORIGINAL RESEARCH

Exosomes Derived From Human Mesenchymal Stem Cells Mitigate Follicular Interstitial Cell Ferroptosis via the miR-26a-5p/PTEN/GPX4 Axis in Rats with Chemotherapy-Induced Premature Ovarian Insufficiency

Juntong Chen[1,*], Xingyu Huo[1,*], Maojiao Qian[1], Qian Xue[1], Yu He[1], Pengzhan Xu[1], Yueming Wang[1], Xiaoxuan Tang[1], Qianqian Luo[1], Hongchu Bao[2,3], Yanlian Xiong[1]

[1]Xu Rongxiang Regenerative Medicine Research Center, Binzhou Medical University, Yantai, People's Republic of China; [2]Reproductive Medicine Centre, The Affiliated Yantai Yuhuangding Hospital of Qingdao University, Yantai, People's Republic of China; [3]Shandong Provincial Key Medical and Health Laboratory of Reproductive Health and Genetics, The Affiliated Yantai Yuhuangding Hospital of Qingdao University, Yantai, People's Republic of China

*These authors contributed equally to this work

Correspondence: Yanlian Xiong; Hongchu Bao, Email xyl8807@163.com; baohongchu@163.com

Background: Premature ovarian insufficiency (POI) is a persistent condition in young women characterized by early follicular development disorders and reduced fertility. Research has found that exosomes derived from human umbilical mesenchymal stem cells (hUCMSC-Exo) have significant tissue repair effects. This study aims to investigate the therapeutic effect and potential molecular mechanism of hUCMSC-Exo on POI.

Methods: In vivo experiments were conducted by intraperitoneally injecting the chemotherapy drug cyclophosphamide (CTX) to establish a 14-day POI rat model. Serum hormone levels were measured using an enzyme-linked immunosorbent assay, and changes in ovarian tissue structure were analyzed using hematoxylin-eosin (HE) staining. Perls staining and transmission electron microscopy were used to assess changes in ovarian ferroptosis. In vitro experiments involved exposing theca interna cells (TICs) treated with CTX to normal and miR-26a-5p inhibitor-treated hUCMSC-Exo. The expression changes of PTEN, Nrf2, and GPX4, which are associated with ferroptosis, were analyzed using immunofluorescence, Western blot, and quantitative reverse-transcription polymerase chain reaction.

Results: hUCMSC-Exo intervention can significantly repair the ovarian tissue structure and functional abnormalities in the model rats, especially ferroptosis. Further bioinformatics analysis revealed that the inhibition of the PTEN/GPX4 pathway-mediated ferroptosis in TICs might be the main mechanism through which exosomes exert their regulatory/therapeutic effects. In vitro experiments, where exosome miR-26a-5p was inhibited, further confirmed that the delivery of miR-26a-5p is crucial for the regulatory effect of exosomes.

Conclusion: In conclusion, our results suggest that hUCMSC-Exos alleviates POI-related dysfunction of ovarian structure and function. The mechanism could be related to the transfers of miR-26a-5p and suppression of PTEN/GPX4 axis signaling-mediated autophagy of TICs. It provides a new perspective for developing treatment methods for patients with metabolic abnormalities related to POI.

Keywords: POI, miR-26a-5p, GPX4, TICs, ferroptosis, hUCMSC-Exo

Introduction

POI is a common reproductive condition in women under 40 years old, characterized by follicular atresia, oligomenorrhea, and increased plasma levels of follicle-stimulating hormone (FSH), which leads to reduced ovarian function.[1] The investigation into employing multiple mesenchymal stem cells (MSCs) to enhance ovarian function in POI models has yielded satisfactory results.[2–4] Current studies show that iron deposition in ovarian tissue can be inhibited by human

Received: 17 April 2025
Accepted: 13 August 2025
Published: 22 August 2025

Graphical Abstract

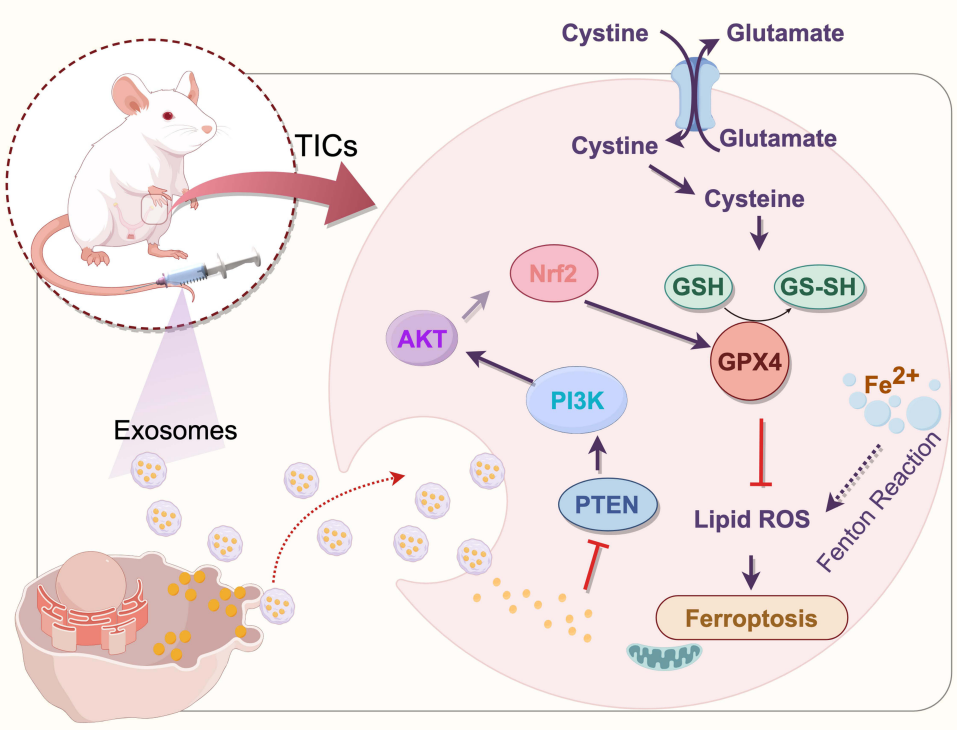

umbilical cord mesenchymal stem cells, which lessens the effect on POI ovarian function.[5] Nonetheless, there is still much to learn about the process and possible targets of human umbilical cord mesenchymal stem cells in the management of POI.

The numerous causes of POI include genetic, autoimmune, and iatrogenic factors.[6] Chemotherapy drugs such as CTX frequently induce early primordial follicle activation and premature follicular pool depletion in a dose-and-time-dependent manner, causing severe ovarian damage.[7] Studies have shown that metabolic abnormalities such as oxidative stress damage, immune homeostasis imbalance, and autophagy in ovarian tissue cells are closely related to the development of POI. Zhu et al reported that the FOXO1-mediated oxidative damage to ovarian tissue is a potential factor leading to POI.[8] Luo et al found that ATG14-mediated granulosa cell autophagy is also involved in POI.[9] Single-cell RNA sequencing and bioinformatics analysis reveal that immune imbalance contributes to the development of POI.[10,11] In addition, ferroptosis, a novel form of programmed cell death characterized by iron overload and lipid peroxidation, is believed to be directly associated with abnormal reproductive ability during POI.[12] In a recent study, Wang et al showed that BNC1 deficiency-triggered ferroptosis through the NF2-YAP pathway induces primary ovarian insufficiency.[13] Hu et al reported that CSE1L can contribute to the cytoplasmic transport-mediated ferroptosis of human ovarian granulosa cells.[14] As a pivotal regulator of folliculogenesis and steroidogenesis, theca interstitial cells (TICs) enhance follicular sensitivity to gonadotropins through secreting androgens (androstenedione) and growth factors (VEGF, IGF-1).[11] TICs dysfunction leads to decreased androgen supply, disrupting estrogen synthesis in GCs and triggering follicular atresia. This hormonal cascade contributes to POI, where follicular developmental arrest prevails.[15] However, it has not been reported whether TICs suffer from structural dysfunction mediated by ferroptosis during POI.

Exosomes are microscopic vesicles with a diameter of 30 to 150 nm that can carry a range of bioactive materials, including lipids, proteins, and nucleic acids.[16,17] Recent studies have shown that hUCMSC-Exos can improve ovarian reserve and regulate hormone levels in cyclophosphamide-treated POI mice.[18] In addition, Ding et al found that hUMSC-Exos reduced ROS formation by targeting the miR-17-5P/SIRT7 pathway and enhanced the proliferation of CTX-damaged ovarian tissue in POI mice.[19] Additionally, Zhou et al have demonstrated that hUCMSC-Exos improves mice's

ovarian function, lowers lipid peroxidation and iron overload-related ovarian tissue damage, and prevents granulosa cell ferroptosis via the Nrf2/GPX4 pathway.[20] Nevertheless, the potential molecular processes by which hUCMSC-Exos regulate the ferroptosis of crucial cellular components in ovarian tissue, such as TICs and GCs, subsequently affect cellular metabolism and function during the POI process have yet to be fully understood.

Thus, we aim to reveal whether hUCMSC-Exo intervention can regulate the imbalance of redox metabolism of TICs, thereby suppressing the cell ferroptosis, and clinically alleviating ovarian structural and functional abnormalities during POI.

Materials and Methods

Reagents

The anti-cancer chemotherapy drug CTX was purchased from Meilun Biotechnology (MB1315-1, Meilunbio, Dalian, China). Phosphoramide mustard (HY-137316A) was purchased from MCE Corporation. Antibodies against PTEN (#10047-1-AP), Nrf2 (#16396-1-AP), GPX4 (#67763-1-lg), FSHR (#22665-1-AP), Cyp17a1 (#14447-1-AP) and GAPDH (#60004-1-lg) were obtained from Proteintech (Wuhan, China). Antibodies against CD63 (#55051), CD9 (#98327), and HSP70 (#4872) were obtained from CST corporation (Danvers, MA, USA). Dil (#BES2087CIMG) was obtained from BIOESN (Shanghai, China). Annexin V-FITC/PI apoptosis assay kit (#Abs50001) was obtained from Absin (Shanghai, China).

Animal Models

Seven-week-old Wistar female rats were bred and maintained under pathogen-free conditions and sterilized water and food (purchased from Ji nan Pengyue Laboratory Animal Breeding Company). This study was performed following protocols approved by the Binzhou Medical University Institutional Animal Care and Use Committee (no. 2023–24). The rats were divided into four groups (n=12/group): Control group, POI group, POI+PBS group, and POI+Exo group. Rats were intraperitoneally injected with 50 mg/kg CTX on the first day and then with 8 mg/kg/d CTX consecutively for 14 days as described in the literature.[21] Rats in the PBS group received 150 μL of PBS via the tail vein on days 15, 18 and 21, while rats in the hUCMSC-Exos group received 150 μL of PBS containing 150 μg of hUCMSC-Exos through the tail vein as described in the literature.[22] Lastly, 7 days after the transplantation of hUCMSC-Exos and PBS, serum, and ovaries were collected and tested for hormone levels, ovarian parameters, and ovarian function-related indices after euthanizing the rat.

Isolation and Identification of hUCMSC-Exos

A culture medium of hUCMSCs at the 3 to 5 passage was obtained. The collected medium was centrifuged at 200×g for 30 min at 4°C. The mixture was diluted with vex exosome isolation reagent (R601, vazyme, China) and kept overnight at 4°C. The collected supernatant was centrifuged at 10,000×g for 1 h at 4°C, and the particles were diluted in PBS and stored at −80°C or used immediately. The separated exosomes were detected by transmission electron microscopy (TEM) (Jeol JEM-1230, Tokyo, Japan), nanosight analysis (Malvern Instruments, Malvern, UK), and Western blot.

Hematoxylin–Eosin Staining

The ovaries were harvested, washed with PBS, fixed in 4% paraformaldehyde (P1110, Solarbio, Qingdao, China), and paraffin-embedded as usual. Four-micron-thick sections of the organs were cut and stained with hematoxylin and eosin (H&E) for histological examination. Ovarian morphology was observed using an optical microscope, and the number of ovaries and follicles was assessed blindly using a histological scoring system from previous studies.[23]

Western Blot Analysis

Previously published methods were followed for Western blot analysis.[24] A developer (NCI4106, Pierce, Rockford, IL, USA) was used to visualize the protein bands. Images were quantified by ImageJ analysis software (National Institutes of Health, Bethesda, MD, USA).

Quantitative Reverse-Transcription PCR (qRT-PCR)

The mRNA levels were determined using a qRT-PCR technique. The miRNA and mRNA expression levels were analyzed using the $2^{-\Delta\Delta CT}$ method and normalized to those of U6 and GAPDH, respectively. Primer information is provided in Supplementary Table 1.

Isolation and Culture of TICs

According to our previous approach,[23] female rats of three weeks of age were anesthetized and euthanized to obtain ovaries. TICs were isolated by puncturing the follicles within the ovaries under a stereomicroscope. The collected cells were digested in collagenase II (2275MG100, BioFroxx, Guangzhou, China) for 45 min and cultured in complete McCoy 5A medium (PM150710, Procell, Wuhan, China) supplemented with 10% fetal bovine serum (#164210, Procell, Wuhan, China) and 1% penicillin-streptomycin (PB180120, Procell, Wuhan, China) at 37°C and 5% CO_2.

In vivo Tracking

Wistar rats were injected with a 150 μL PBS solution containing 150 μg of hUCMSC-Exos via the tail vein. The control group received a 300 μL injection of PBS. After 48 hours, abdominal and lateral imaging were performed with the IVIS lumina III system (PerkinElmer, UK).

Perls Staining

According to the ferrous staining kit (G3320, Solarbio, Beijing, China) protocol, ovarian tissue paraffin sections (5 μm) were baked at 60°C for 3 hours, dewaxed in xylene, and rehydrated to water by graded alcohol. Then the sections were immersed in the ferrous staining working solution for 30 min, and then washed thoroughly with distilled water and stained with nuclear fast red solution for 5 min. Finally, the slides were dehydrated through graded alcohols, clarified in xylene, and mounted in neutral resin for microscopic examination.

Apoptosis Assay

Cells were treated with 40 μM of CTX for 24 h, and then the cells were digested and gently resuspended in a staining buffer containing 5 μL Annexin V-FITC storing solution and 10 μL storing propidium iodide solution according to the instructions of Annexin V-FITC detection Kit (abs50001, Absin, China); after that, the cells were incubated for 20 min in the dark at 4 °C. At the end of incubation, the cells were detected by flow cytometry.

Functional Annotation and miRNA Target Prediction

Gene Ontology (GO) and Kyoto Encyclopedia of Genes and Genomes (KEGG) enrichment analyses were performed through the online platform https://www.bioinformatics.com.cn/ to annotate the biological functions and signaling pathways of the screened genes. For miRNA target prediction, a combinatorial approach was employed using the following databases: TargetScan (https://www.targetscan.org/vert_80/), miRDB (https://mirdb.org/), miRWalk (http://mirwalk.umm.uni-heidelberg.de/), ENCORI/starBase (https://rnasysu.com/encori/index.php). Overlapping targets identified across all four databases were retained as high-confidence miRNA-mRNA interactions.

Statistical Analysis

Statistical analysis was performed using GraphPad Prism 9.0 analysis software. Descriptive statistics (mean ± SD) are reported for gonadal hormone levels (AMH, FSH, LH, E_2). All cell experiments were performed in triplicate at least. Significant differences were determined by the independent Student's *t*-test between the two groups, while one-way ANOVA analysis was performed to compare multiple groups. $p < 0.05$ was considered statistically significant.

Other detailed methods are available in the Supplementary Material 1: Detailed Methods.

Results

Characterization and Analysis of hUCMSC-Exos

TEM and NTA exhibited that hUCMSC-Exos were bilayer vesicle structures with a diameter of 80–200 nanometers (Figure 1A and B). Western blotting confirmed the high expression of CD63, CD9, and HSP70 in hUCMSC-Exos (Figure 1C). Following the tail vein injection of Dil-labeled hUMSC-Exos, in vivo tracking revealed a high accumulation of hUMSC-Exos in the thoracic and abdominal regions as well as in both ovaries of the rats (Figure 1D). Further immunofluorescence staining of the TICs marker Cyp17a1 indicated significant overlap between Dil-labeled exosomes and Cyp17a1 in rat ovarian tissue, particularly within the TICs (Figure 1E and F). These findings indicated that hUCMSC-Exos have ovarian tropism in vivo and can be taken up by TICs.

hUCMSC-Exos Improved the Ovarian Morphological and Functional Abnormalities of POI Rats

As shown in Figure 2A, the POI model was established by injecting CTX intraperitoneally, and then evaluating the efficacy of tail vein intervention with equal parts hUCMSC-Exos and PBS. Compared with the control group, the POI group rats showed significantly slower weight gain and lower ovarian index. On the contrary, POI rats showed a significant increase in body weight and ovarian index after treatment with hUCMSC-Exos compared with PBS (Figure 2B and C). H&E staining

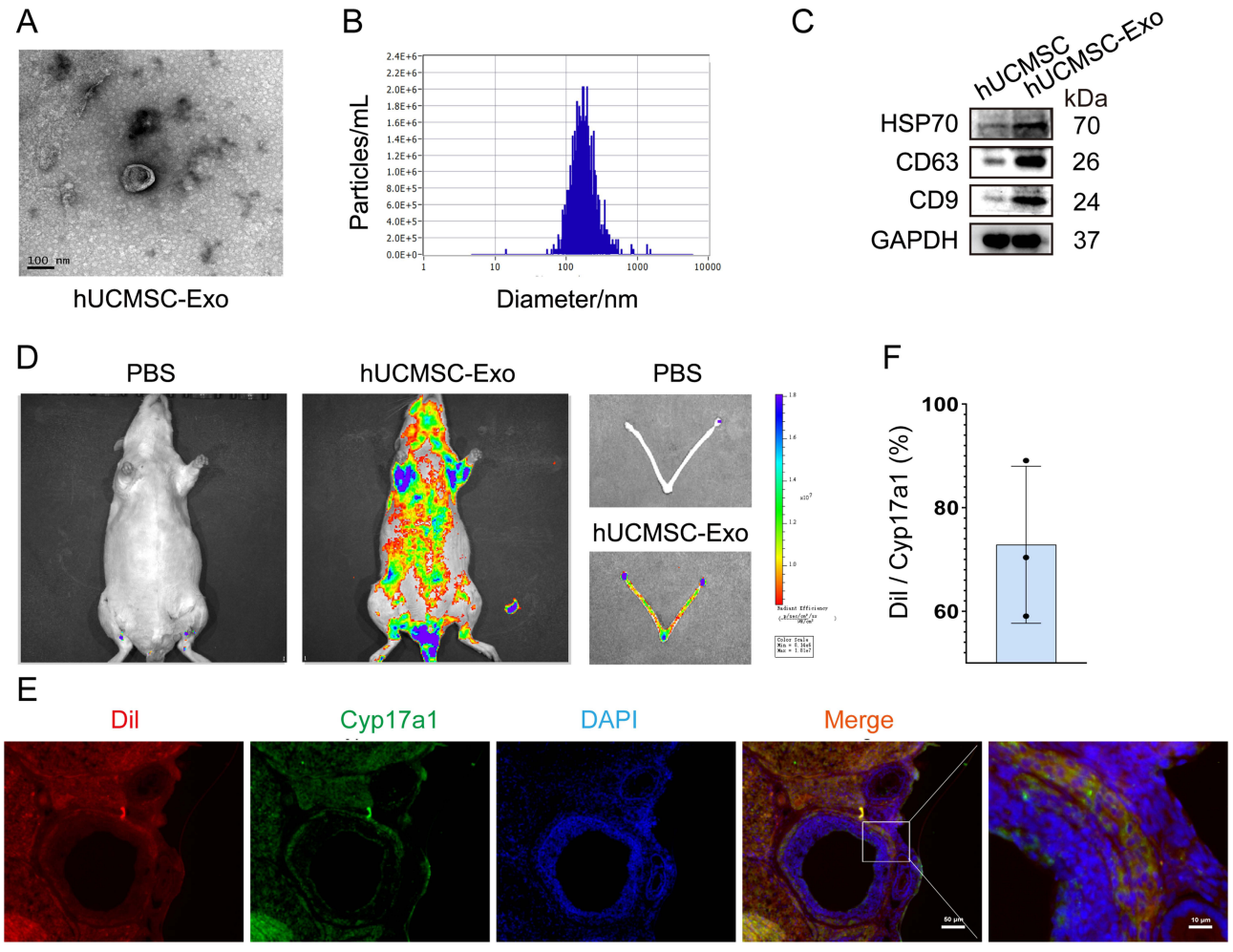

Figure 1 Characterization and analysis of hUCMSC-Exos. (**A**) The microscopic structure of hUCMSC-Exos was verified by TEM. (**B**) Diameter of hUCMSC-Exos by NTA. (**C**) The markers were evaluated by Western blotting. (**D**) Dil-labeled exosome-injected rats were utilized for in vivo tracking. (**E**) Ovaries injected with Dil-labeled exosomes were stained with immunofluorescence (scale bar =50 μm; scale bar =10 μm). (**F**) Quantitative analysis of Dil/Cyp17a1.

https://doi.org/10.2147/IJN.S532207

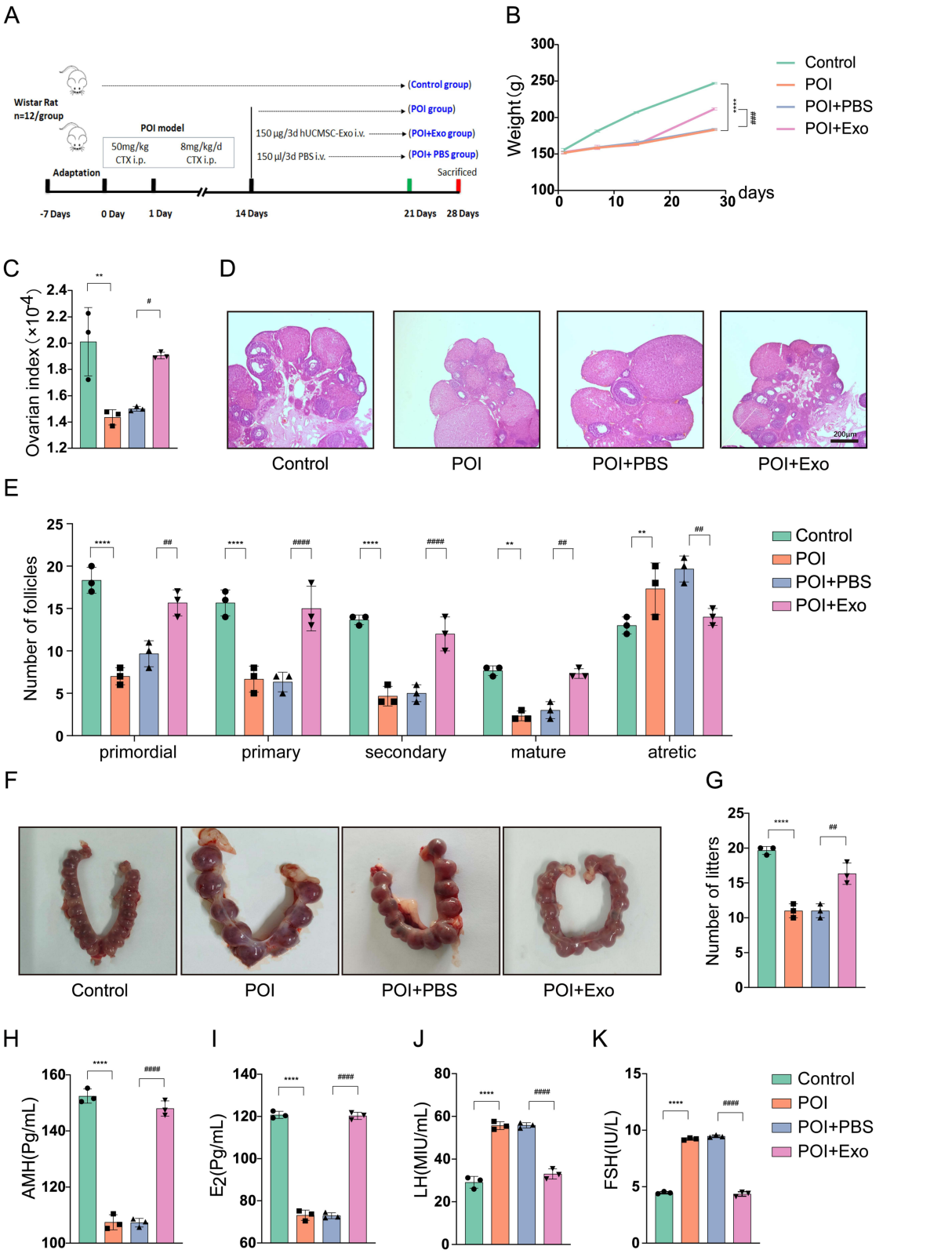

Figure 2 hUCMSC-Exos improved the ovarian morphological and functional abnormalities of POI rats. (**A**) Schematic diagram of animal model. (**B**) Body weight of control, POI, POI+PBS, POI+Exo groups. (**C**) Ovarian index of control, POI, POI+PBS, POI+Exo groups. (**D**) H&E staining of control, POI, POI+PBS, POI+Exo groups (scale bar = 200μm). (**E**) Number of follicles in the groups of control, POI, POI+PBS, and POI+Exo groups. (**F** and **G**) Number of litters in the groups of control, POI, POI+PBS, and POI +Exo groups. (**H-K**) Measurement of the hormone levels of AMH, E_2, LH, and FSH. The data are presented as the means ± SD of at least three independent experiments. **p < 0.01, ****p < 0.0001, the control group vs the POI group; #p < 0.05, ##p < 0.01, ###p< 0.001, #####p < 0.0001, the POI+PBS group vs the POI+Exo group.

revealed that the number of primordial follicles, primary follicles, secondary follicles, and mature follicles in POI rats was significantly less than that in the control group. After hUCMSC-Exos treatment, the number of follicles was significantly increased and the atretic follicles were reduced compared to the POI+PBS group (Figure 2D and E). In addition, the results of the cage experiment showed that compared with the control group, the number of embryos in the POI group was significantly reduced, while exosome therapy could significantly increase the number of embryos (Figure 2F and G). Furthermore, the POI group had significantly higher levels of LH and FSH than the control group, but significantly lower levels of AMH and E_2. The POI rats' aberrant hormone levels were considerably normalized after receiving hUCMSC-Exos therapy (Figure 2H–K). The above findings suggested that in vivo administration with hUCMSC-Exos reduces ovarian morphological and functional abnormalities while improving reproductive ability in POI rats.

hUCMSC-Exos Intervention Inhibits Ferroptosis in Ovarian Tissue of POI Rats

Next, we measured the degree of ferroptosis-related indicators in the ovarian tissue of POI rats. As shown in Figure 3A and B, Perls staining results showed that compared with the control group, there were significantly higher ferrous positive areas (blue) in the ovarian tissue of POI group rats. In addition, compared with the control group, the GSH/GSSG ratio was significantly reduced, and the MDA level was significantly increased in the ovarian tissue of POI group rats (Figure 3C and D). Furthermore, TEM revealed that the mitochondrial morphology remained intact in the control group, whereas the mitochondrial cristae of ovarian TICs in POI rats were fragmented and disordered, and accompanied by vacuolar formation (Figure 3E). Meanwhile, compared with the PBS treatment group, hUCMSC-Exos treatment can significantly upregulate the GSH/GSSG ratio, downregulate MDA levels and ferrous positive areas, and alleviate TICs mitochondrial damage. The above findings suggested that in vivo administration with hUMSC-Exos inhibits ferroptosis in the ovarian tissue of POI rats.

miR-26a-5p Is Abundant in hUCMSC-Exos and Targets PTEN

miRNA-seq was utilized to screen miRNAs to evaluate the miRNA expression profile of hUCMSC-Exos and the therapeutic mechanism (GSE159814). As shown in Figure 4A, the top ten most abundant miRNAs were hsa-miR-21-5p, hsa-miR-24-3p, hsa-miR-22-3p, hsa-miR-26a-5p, hsa-miR-146a-5p, hsa-miR-221-3p, hsa-let-7a-5p, hsa-miR-29a-3p, hsa-miR-100-5p, hsa-miR-125b-5p, accounting for almost 55% of the total miRNAs. The miR-26a-5p target genes were predicted and intersected by four databases, TargetScan, miRWalk, starBase, and miRDB, and a total of 260 genes were identified (Figure 4B). KEGG enrichment analysis of the collected target genes revealed that the phosphatidylinositol signaling system, cellular senescence, and mTOR signaling pathway were the main pathways affected (Figure 4C). Next, we conducted that PTEN was produced by intersection analysis of the 264 ferroptosis up-regulation genes in the FerrDb (http://www.zhounan.org/ferrdb/current/), 1188 POI-related genes in the Gene Card (https://www.genecards.org/), and the 260 miR-26a-5p target genes (Figure 4D). Additionally, we used a dual-luciferase reporter assay to locate the binding site of miR-26a-5p in PTEN, which was predicted by TargetScan (Figure 4E). Compared to the control, treatment with the miR-26a-5p mimic decreased luciferase activity, while treatment with the miR-26a-5p inhibitor significantly increased the relative luciferase activity. Moreover, when the seed sequence of the miR-26a-5p binding region was altered, no effect of miR-26a-5p on luciferase activity was detected (Figure 4F). Aiming to validate the relationship between miR-26a-5p and the PTEN/GPX4 axis, it was detected intracellular PTEN expression changes in vitro theca cells under miR-26a-5p knockdown and overexpression interventions. The qRT-PCR demonstrated that compared with the mimics negative control (mimics NC), intervention with miR-26a-5p mimics significantly downregulated PTEN expression in theca cells. Conversely, compared with the inhibitor negative control (inhibitor NC), miR-26a-5p inhibitor intervention significantly upregulated PTEN expression in theca cells (Figure 4G). The qRT-PCR confirmed that miR-26a-5p expression was significantly less in the POI group compared to the control, but increased with hUCMSC-Exos treatment (Figure 4H). Meanwhile, PTEN mRNA expression significantly decreased in the ovaries of POI rats after hUCMSC-Exos transplantation (Figure 4I). These results suggest that miR-26a-5p derived from hUCMSC-Exos may affect the ferroptosis process of ovarian tissue by targeting PTEN during POI.

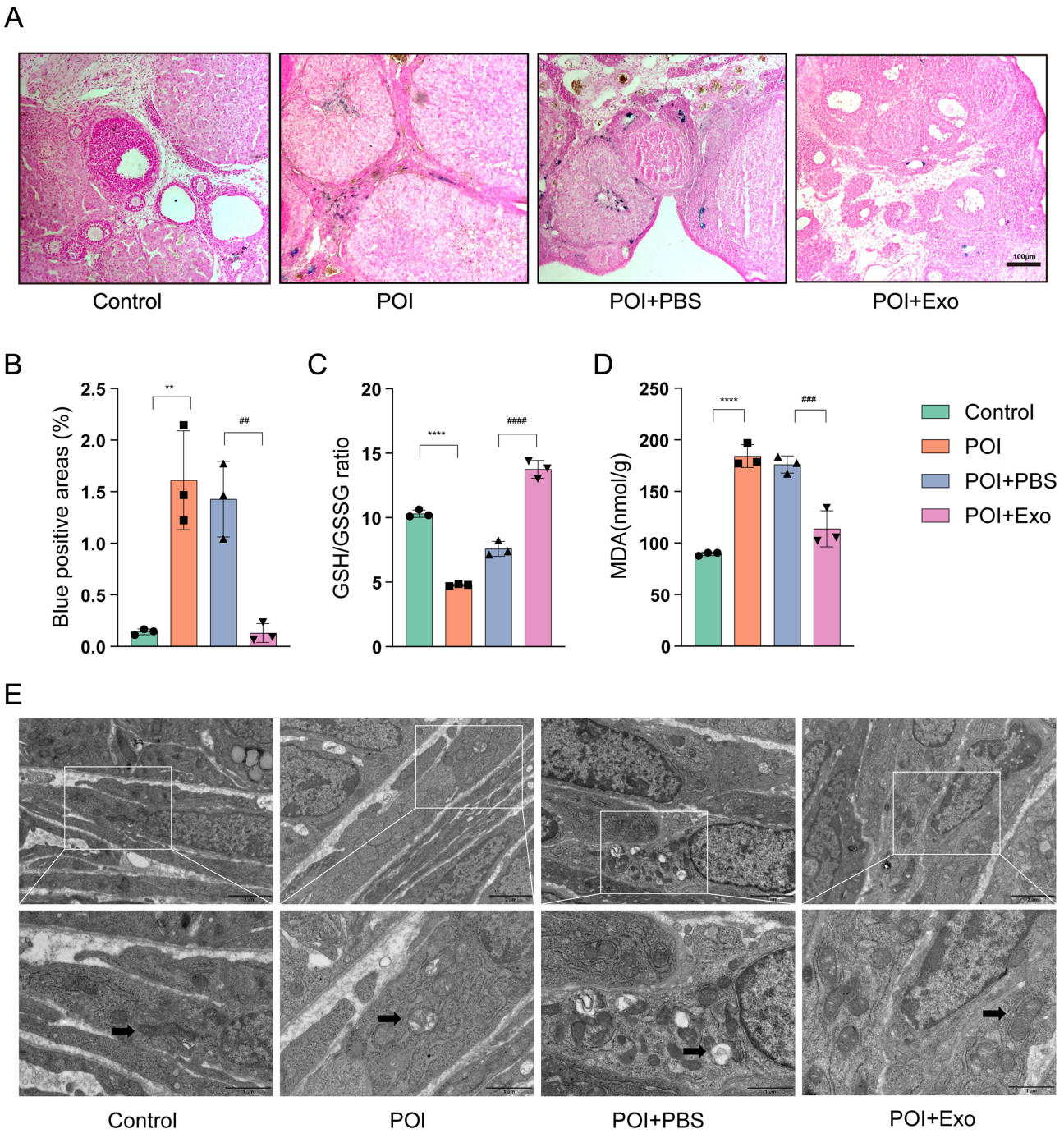

Figure 3 hUCMSC-Exos intervention inhibits ferroptosis in ovarian tissue of POI rats. (**A** and **B**) Perls staining illustrates the expression of Fe^{2+} content, the nucleus is represented by the red section and Fe^{2+} by the blue section (scale bar = 100 μm). (**C**) Measurement of GSH/GSSG in Control, POI, POI+PBS, POI+Exo groups. (**D**) Measurement of MDA in Control, POI, POI+PBS, POI+Exo groups. (**E**) Representative images of mitochondrial ultrastructure of TICs with TEM (scale bar = 2 μm; scale bar = 1 μm), the arrow points to the mitochondrion. The data are presented as the means ± SD of at least three independent experiments. $^{**}p < 0.01$, $^{****}p < 0.0001$, the control group vs the POI group; $^{\#\#}p < 0.01$, $^{\#\#\#}p < 0.001$, $^{\#\#\#\#}p < 0.0001$, the POI+PBS group vs the POI+Exo group.

hUCMSC-Exos Alleviates Ferroptosis of Ovarian Tissue by Targeting the PTEN/GPX4 Pathway

Fresh ovarian tissue was utilized to investigate the mechanism of hUCMSC-Exos regulating ferroptosis in ovarian tissue by targeting the PTEN/GPX4 pathway. As shown in Figure 5A–D, Western blotting showed that compared with the control group, the expression of PTEN was significantly increased, and the Nrf2 and GPX4 levels were significantly

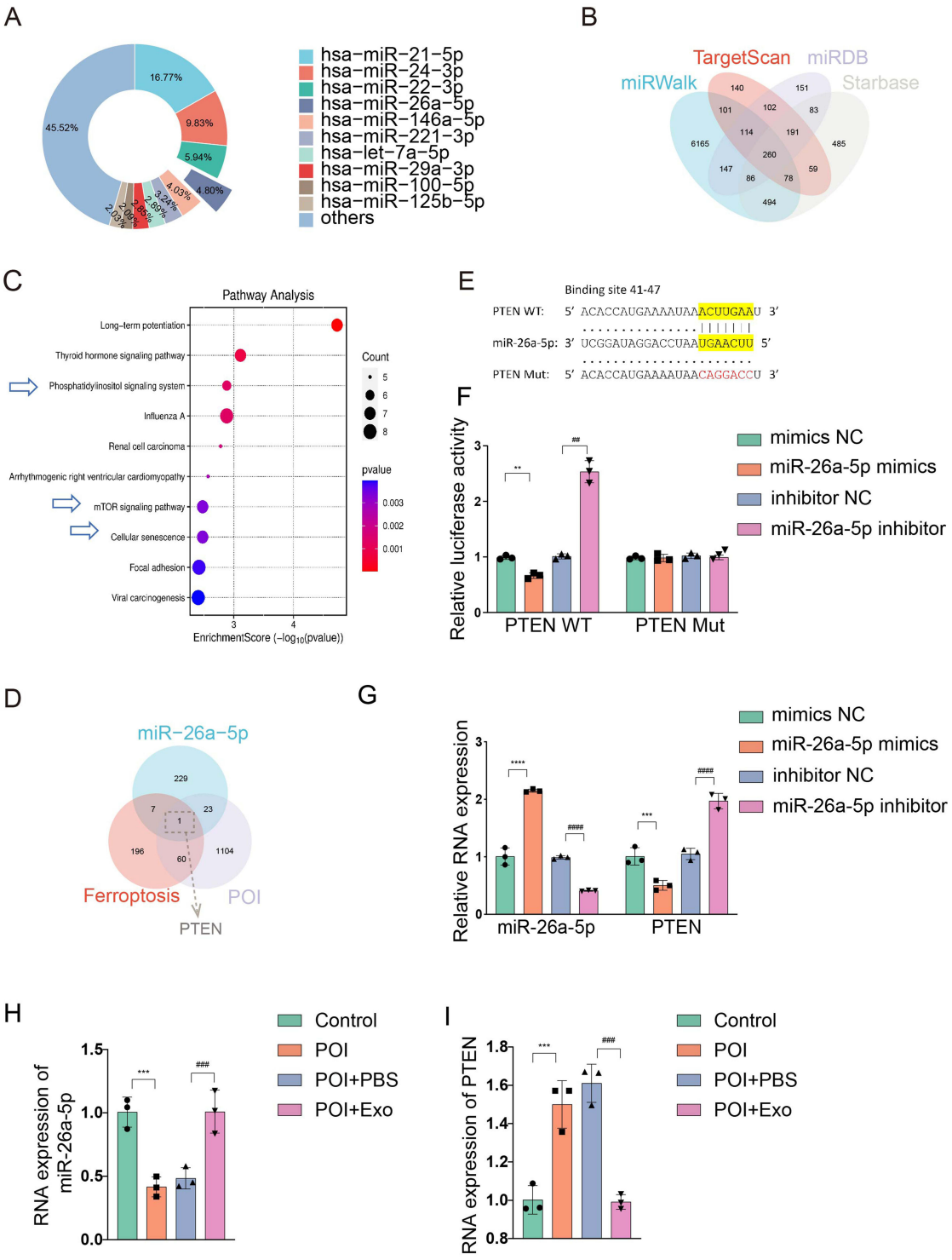

Figure 4 miR-26a-5p is abundant in hUCMSC-Exos and targets PTEN. (**A**) miRNAs were abundantly expressed in hUCMSC-Exos. (**B**) Target gene intersection analysis for miR-26a-5p. (**C**) Evaluation of the Target Gene Enrichment Pathway for miR-26a-5p, the blue arrows point to the key pathways indicating protein phosphorylation. (**D**) Analysis of intersections among POI-related genes, miR-26a-5p target genes, and ferroptosis-activated gene libraries. (**E** and **F**) Binding site prediction of miR-26a-5p in the 3′-UTR of PTEN using TargetScan and Luciferase activity was measured by a dual-luciferase reporter gene assay, the yellow highlight shows the region on the mRNA of the PTEN gene that binds to miR-26a-5p, the red text shows that in the PTEN Mut sequence; the nucleotide sequence of the original binding region with miR-26a-5p has changed to "CAGGACCU", $^{**}p < 0.01$, the mimics NC group vs the miR-26a-5p mimics group; $\#\#p < 0.01$, the inhibitor NC group vs the miR-26a-5p inhibitor group. (**G**) The relative RNA expression of miR-26a-5p and PTEN. $^{***}p < 0.001$, $^{****}p < 0.0001$, the mimics NC group vs the miR-26a-5p mimics group; $\#\#\#\#p < 0.0001$, the inhibitor NC group vs the miR-26a-5p inhibitor group. (**H**) The expression of miR-26a-5p. $^{***}p < 0.001$, the control group vs the POI group; $\#\#\#p < 0.001$, the POI+PBS group vs the POI+Exo group. (**I**) The mRNA levels of PTEN were evaluated by qRT-PCR. $^{***}p < 0.001$, the control group vs the POI group; $\#\#\#p < 0.001$, the POI+PBS group vs the POI +Exo group. The data are presented as the means ± SD of at least three independent experiments.

https://doi.org/10.2147/IJN.S532207

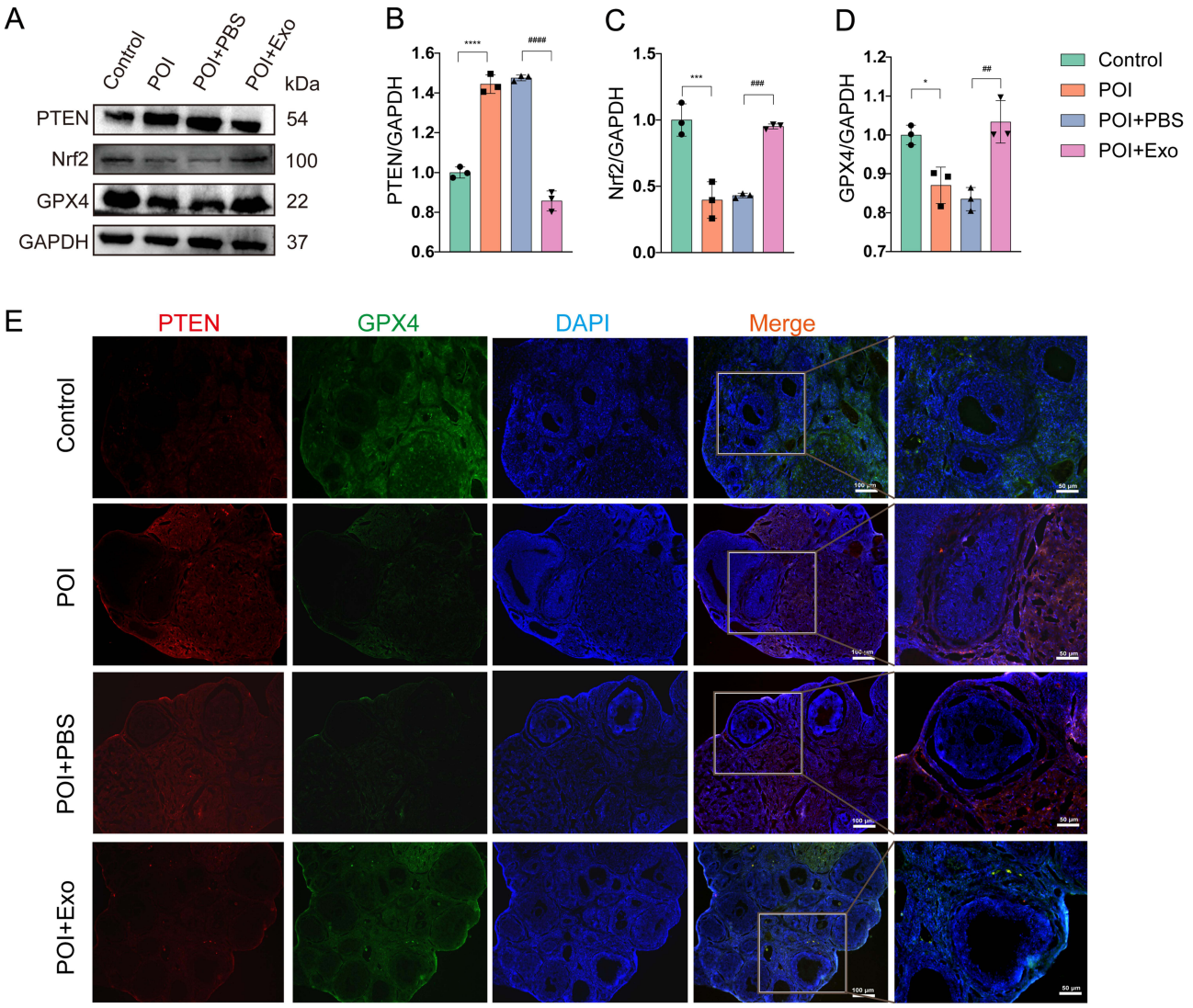

Figure 5 hUCMSC-Exos alleviates ferroptosis of ovarian tissue by targeting the PTEN/GPX4 pathway. (**A**) Western blotting identified the PTEN/GPX4 axis protein alterations. (**B**) The protein level of PTEN. (**C**) The protein level of Nrf2. (**D**) The protein level of GPX4. (**E**) The expression of PTEN and GPX4 was tested by immunofluorescence staining. Red represents PTEN, green represents GPX4, and The nucleus was stained with DAPI (blue). The data are presented as the means ± SD of at least three independent experiments. *$p < 0.05$, ***$p < 0.001$,****$p < 0.0001$, the control group vs the POI group; ##$p < 0.01$, ###$p < 0.001$, ####$p < 0.0001$, the POI+PBS group vs the POI+Exo group.

reduced in the ovarian tissue of POI group rats. Compared with the PBS group, hUCMSC-Exos treatment can significantly downregulate the protein expression of PTEN and upregulate the protein expression of Nrf2, and GPX4. Furthermore, immunofluorescence staining revealed that the analysis results of molecules PTEN and GPX4 were consistent with the above results and expressed in TICs (Figure 5E). These findings suggested that hUCMSC-Exos alleviates ferroptosis of ovarian tissue by targeting the PTEN/GPX4 pathway.

Characterization of TIC

To explore the molecular mechanism of hUCMSC-Exos regulating ferroptosis of TICs, TICs were isolated from the ovarian tissue of rats. As shown in Figure 6A, the cells were spindle-shaped under the light microscope. Furthermore, immunofluorescence staining shows that FSHR was negative and Cyp17a1 was positive. It was determined that the isolated cells were TICs (Figure 6B). Next, the suitable CTX concentration (40 μM) was determined using the CCK-8 assay to create an in vitro damage model (Figure 6C). Dil labeling was seen in TICs when they were co-cultured with hUCMSC-Exos, suggesting that the TICs internalized the hUCMSC-Exos (Figure 6D).

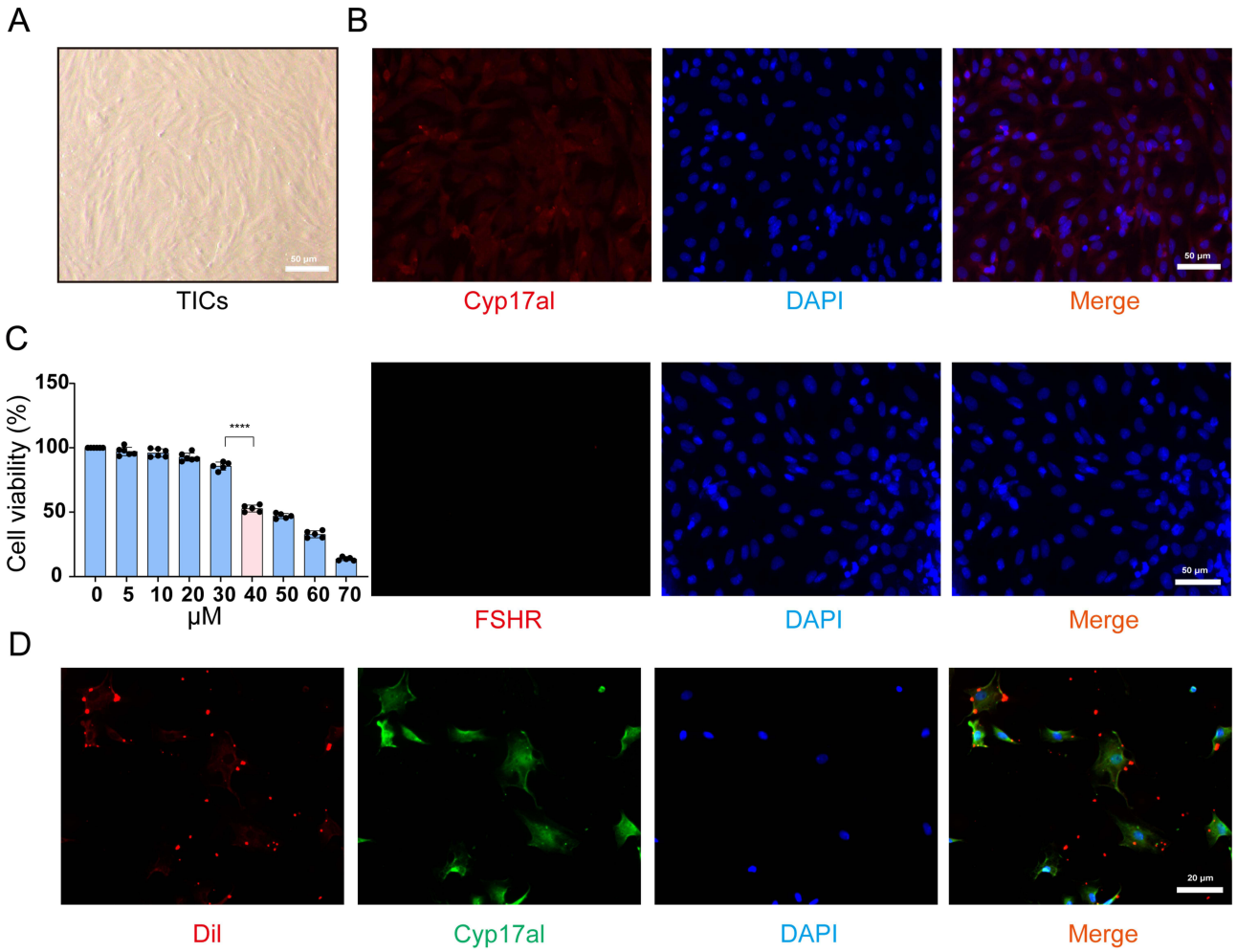

Figure 6 Characterization of TICs. (**A**) The typical fibroblastic morphology of TICs was verified by microscopy (scale bar = 50 μm). (**B**) Immunofluorescence staining tested the expression of Cyp17al and FSHR (scale bar = 50 μm). (**C**) cck-8 detects the toxicity of CTX to TICs. (**D**) Endocytosis in exosomes was detected by immunofluorescence staining (scale bar = 20 μm). The data are presented as the means ± SD of at least three independent experiments. ****$p < 0.0001$, 30μM vs 40μM.

hUCMSC-Exos Prevented Ferroptosis in TICs via the PTEN/GPX4 Pathway in vitro

To further explore the mechanism of hUCMSC-Exos regulating TICs ferroptosis by targeting miR-26a-5p/ PTEN/GPX4 pathway, we co-cultured CTX-induced TICs with hUCMSC-Exos. As shown in Figure 7A and B, flow cytometry was used to examine changes in TICs apoptosis before and after hUCMSC-Exos intervention. The number of apoptotic TICs in the CTX group was significantly more than in the control group, while hUCMSC-Exos therapy could significantly increase the number of TICs. Moreover, compared with the control group, the GSH/GSSG ratio was significantly reduced and the MDA level was significantly increased in the CTX-induced TICs group. After hUCMSC-Exos intervention, the ratio of GSH/GSSG and MDA levels showed opposite results (Figure 7C and D). Compared with the control group, the CTX group TICs showed significantly higher protein expression of PTEN and lower protein expression of Nrf2, and GPX4. In contrast, the levels of these ferroptosis-related proteins showed opposite results in the hUCMSC-Exos treatment group (Figure 7E–H). In addition, the detection of miR-26a-5p and PTEN miRNA /mRNA levels indicated that hUCMSC-Exos intervention significantly upregulated the miR-26a-5p level and significantly downregulated the PTEN mRNA levels in CTX-damaged TICs (Figure 7I and J). Immunofluorescence staining indicated that the ferroptosis-related molecules' analysis results corresponded with the above results (Figure 7K). These results suggested that hUCMSC-Exos prevented ferroptosis in TICs via the PTEN/GPX4 pathway in vitro, potentially involving the transfer of miR-26a-5p.

https://doi.org/10.2147/IJN.S532207

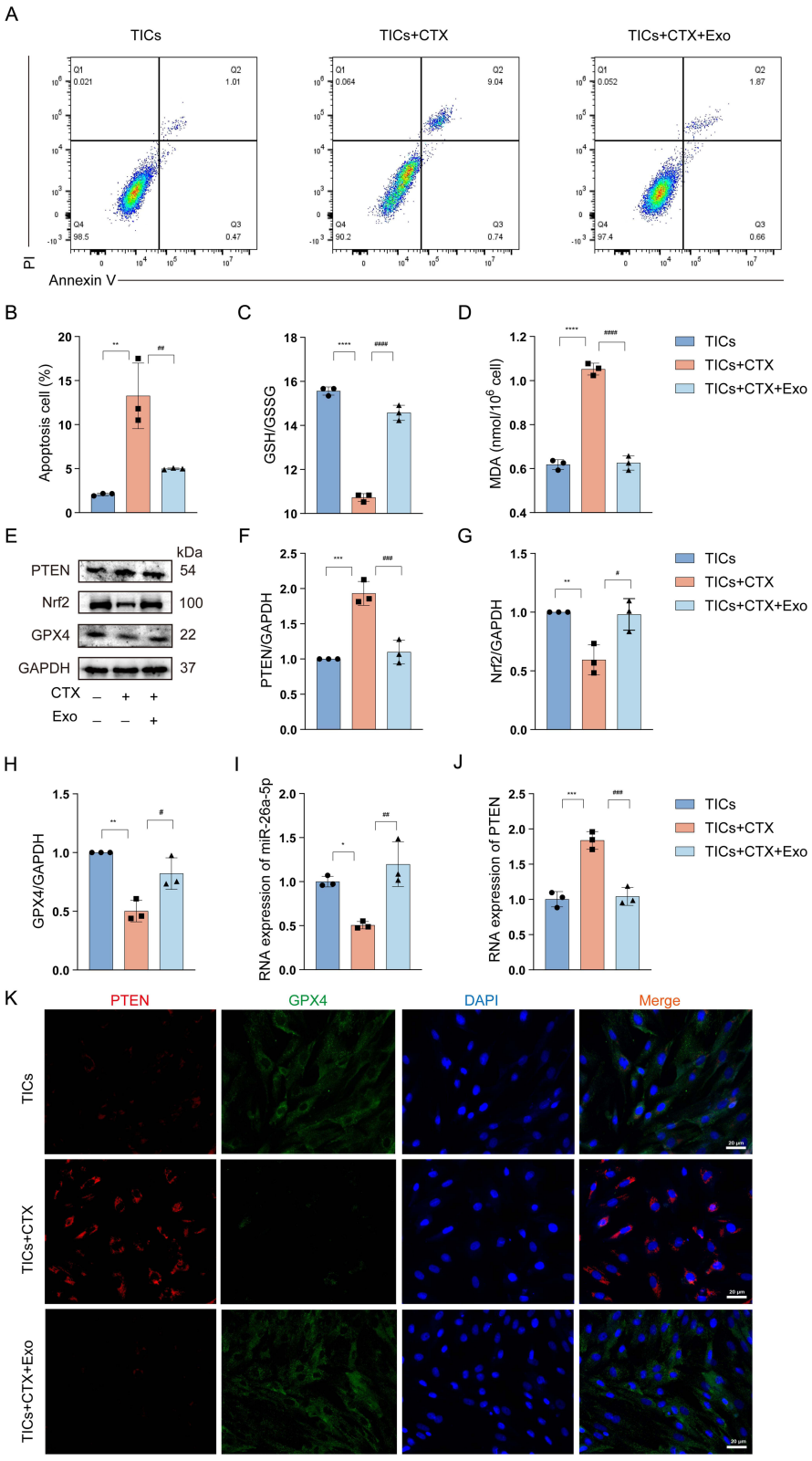

Figure 7 hUCMSC-Exos prevented ferroptosis in TICs via the PTEN/GPX4 pathway in vitro. (**A** and **B**) Flow cytometry analysis of TICs apoptosis after Annexin V/PI staining. (**C** and **D**) The levels of GSH/GSSG and MDA. (**E**) Western blotting identified the PTEN/GPX4 axis protein alterations. (**F**) The protein level of PTEN. (**G**) The protein level of Nrf2. (**H**) The protein level of GPX4. (**I**) The relative miR-26a-5p levels in TICs were evaluated by RT-PCR. (**J**) The RNA levels of PTEN in TICs were evaluated by RT-PCR. (**K**) The expression of PTEN and GPX4 was detected by immunofluorescence staining. Red represents PTEN, green represents GPX4, and blue represents DAPI. The data are presented as the means ± SD of at least three independent experiments. *$p < 0.05$, **$p < 0.01$, ***$p < 0.001$, ****$p < 0.0001$, the TICs group vs the TICs+CTX group; #$p < 0.05$, ##$p < 0.01$, ###$p < 0.001$, #####$p < 0.0001$, the TICs+CTX group vs the TICs+CTX+Exo group.

The Delivery of miR-26a-5p is Key for hUCMSC-Exos to Regulate the Ferroptosis of TICs by Targeting the PTEN/GPX4 Pathway

To examine the above hypothesis, hUCMSCs were treated with miR-26a-5p inhibitor or inhibitor NC. As shown in Figure 8A, qRT-PCR confirmed that the miR-26a-5p levels of hUCMSCs were significantly decreased in the miR-26a-5p inhibitor group. Next, extracted hUCMSC-Exos were co-cultured with CTX-induced TICs, respectively. Compared to the inh NC group, the GSH/GSSG ratio was significantly lower in the miR-26a-5p inhibitor group, while the level of MDA was significantly higher in the miR-26a-5p inh group (Figure 8B and C). In addition, the miR-26a-5p inh group had far fewer surviving tics cells than the inh NC group (Figure 8D and E). Immunofluorescence staining reveals that compared to the inh NC group, PTEN expression markedly increased and GPX4 expression greatly decreased in the miR-26a-5p inhibitor group (Figure 8F). Meanwhile, Western blotting demonstrates that the analysis results of the ferroptosis-related molecules coincide with above results (Figure 8G–J). Additionally, the miR-26a-5p inhibitor group had a significantly greater level of PTEN mRNA and a significantly lower level of miR-26a-5p than the NC group (Figure 8K and L). These results suggested that miR-26a-5p transporting is essential for hUCMSC-Exos to regulate TICs ferroptosis via the PTEN/GPX4 pathway.

Discussion

MSC-Exos have drawn a lot of interest in the treatment of POI because of their capacity to support damaged tissue repair, microenvironment stability, and anti-aging.[25,26] Numerous studies have demonstrated in recent years that hUCMSCs and the exosomes they produce are crucial in controlling the composition and functionality of ovarian tissue cells in women.[27,28] Our research demonstrated that by preventing the ferroptosis of TICs, hUCMSC-Exos reduced ovarian damage in POI rats. Additionally, miR-26a-5p delivered by hUCMSC-Exos, which targets the PTEN/GPX4 pathway, is primarily responsible for inhibiting ferroptosis during POI. It is anticipated that our findings will offer fresh therapeutic targets and approaches for POI clinical treatment.

POI is commonly observed in young women following chemotherapy, although it can also arise from multiple etiologies, including genetic disorders, autoimmune diseases, and idiopathic factors. Chemotherapy-induced ovarian damage remains a major clinical contributor to POI in reproductive-aged women.[29] Lu et al found that CTX affected the mitochondrial function of GCs, resulting in abnormal ovarian function and the emergence of POI.[30] Liu et al discovered that CTX inhibited SIRT1 and PGC-1α activity, which in turn caused activation of the ATM/p53 pathway and accelerated the POI process.[31] In this study, it was observed that the body weight, ovarian index, follicle count, and the number of embryos in the uterine horn were significantly reduced in POI rats, while the number of arrested follicles increased, and serum hormone levels were also significantly decreased. In vitro experiments revealed that, in contrast to the control group, CTX administration triggered an increase in ferroptosis-related molecules in TICs. According to this study, POI may be triggered by ferroptosis in TICs. Mature TICs preserve the integrity of the follicular structure and supply vital nutrients for the ovaries' growth and development.[15] When TICs are disturbed, GCs fail to generate estrogen, and the release of growth factors and androgens is drastically decreased. These results in difficulties with follicular development and POI brought on by atresia. Thus, aberrant TIC metabolism could be a significant initiator of the morphological and functional defects in POI ovaries caused by CTX.

Ferroptosis is the accumulation of intracellular iron overload and lipid peroxides, which is crucial for cell growth, metabolism, and other processes to keep the body in balance and homeostasis.[32,33] It has been extensively researched in several female reproductive problems.[34–36] In this study, we found that the GSH/GSSG ratio in the ovarian tissue and TICs of CTX-induced POI rats was significantly reduced, while lipid peroxide levels were elevated, particularly MDA. Furthermore, CTX causes notable alterations in divalent iron and mitochondrial morphology in TICs, such as outer membrane rupture and cristae blurring. As one of the main signaling pathways for Ferroptosis, the PTEN signaling pathway has drawn a lot of interest. Yang et al discovered that miR-144-5p supplied by BMSC-derived exosomes activate the PTEN/PI3K/AKT pathway, protecting ovarian tissue from damage caused by chemotherapy.[37] Additionally, we discovered that ferroptosis-related molecules such as Nrf2 and GPX4 protein levels were decreased in POI rats. In addition, PTEN is activated while GPX4 expression is inhibited. When GPX4 activity is inhibited, it leads to the accumulation of lipid peroxides, ultimately resulting in

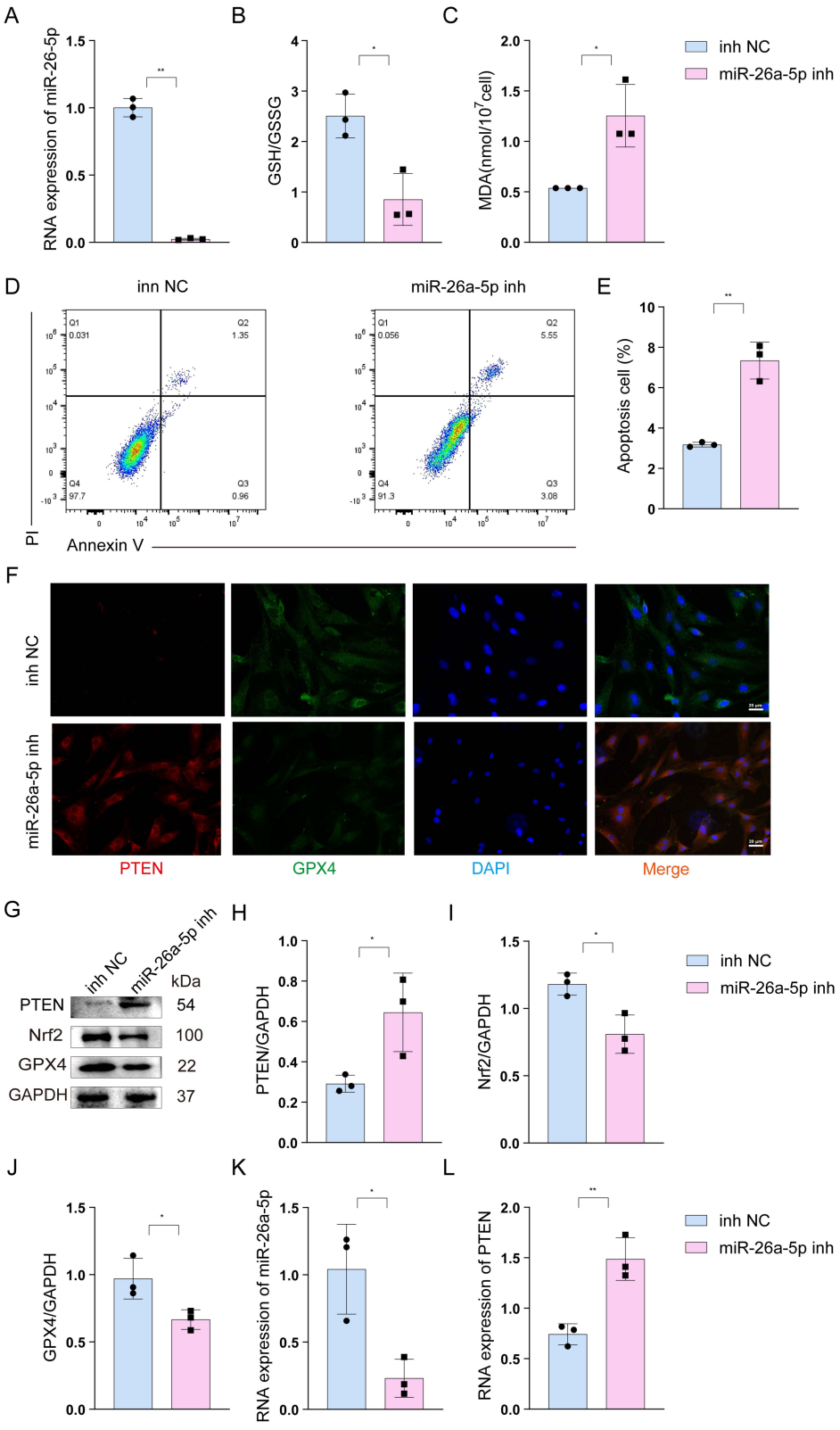

Figure 8 The delivery of miR-26a-5p is key for hUCMSC-Exos to regulate the ferroptosis of TICs by targeting the PTEN/GPX4 pathway. (**A**) The level of miR-26a-5p. (**B** and **C**) The level of GSH/GSSG and MDA. (**D** and **E**) Flow cytometry analysis of TICs apoptosis after Annexin V/PI staining. (**F**) The expression of PTEN and GPX4 was detected by immunofluorescence staining. Red represents PTEN, green represents GPX4, and blue represents DAPI. (**G**) Western blotting identified the PTEN/GPX4 axis protein alterations. (**H**) The protein level of PTEN. (**I**) The protein level of Nrf2. (**J**) The protein level of GPX4. (**K**) The relative miR-26a-5p levels in TICs were evaluated by RT-PCR. (**L**) The RNA levels of PTEN were evaluated. The data are presented as the means ± SD of at least three independent experiments. *$p < 0.05$, **$p < 0.01$, the inh NC group vs the miR-26a-5p inh group.

ferroptosis.[38] Similarly, in vitro experiments have revealed that CTX treatment of TICs elevates ferroptosis-associated markers and indicators, activating the PTEN signaling pathway POI and causing damage to ovarian tissue.

MSC-Exos plays an important role in the transmission of intercellular signaling.[39] MSC-derived exosomes from bone marrow can effectively protect liver cells from ferroptosis by enhancing the activity of the deubiquitinase OTUB1 and maintaining the stability of SLC7A11.[40] hUCMSC-Exos inhibits the expression of divalent metal transporter 1 (DMT1) via miR-23a-3p, thereby alleviating ferritin deposition and protecting cardiomyocytes from damage.[41] We discovered in our research that hUCMSC-Exos promotes follicle development and ovarian function in vivo. Rats in the hUCMSC-Exos group showed lower levels of FSH and LH and greater levels of serum E_2 and AMH than those in the PBS group. Furthermore, the number of embryos in the uterus of POI rats rose following treatment with hUCMSC-Exos, suggesting that ovarian function had recovered. These findings suggest that hUCMSC-Exos intervention can alleviate ovarian structural and functional abnormalities in POI rats and restore reproductive capacity.

Many studies have highlighted the potential of using exosomes derived from MSCs, specifically exosomal miRNAs, to treat various diseases and injuries.[42,43] Xiong et al showed that hUCMSC-Exos delivered miR-16a-5p targeting to ATF6/CHOP pathway, suppressed $CD4^+$ T cells apoptosis, and treated GVHD.[44] Using dual luciferase reporter gene detection and hUCMSC-Exos transcriptome sequencing, we discovered that miR-26a-5p was substantially expressed in hUCMSC-Exos targeting PTEN, a crucial protein controlling the ferroptosis pathway. In vivo, tests demonstrated that hUCMSC-Exos therapy suppressed the expression of markers linked to ferroptosis and markedly raised the amount of miR-26a-5p in ovarian tissue. Furthermore, its regulatory effect on pathways linked to TICs ferroptosis was significantly diminished following the in vitro inhibition of miR-26a-5p exosomes. Our findings highlight the critical role of ferroptosis and miR-26a-5p in modulating TIC function, aligning with previous studies on follicular development. However, the study has limitations: lack of long-term follow-up data and direct clinical validation. Future research should address these gaps to enhance translational potential. Besides, our study demonstrated the efficacy of exosomes at a single time point post-injection. However, the lack of time-course analysis limits our understanding of the dynamic effects and underlying mechanisms. Future

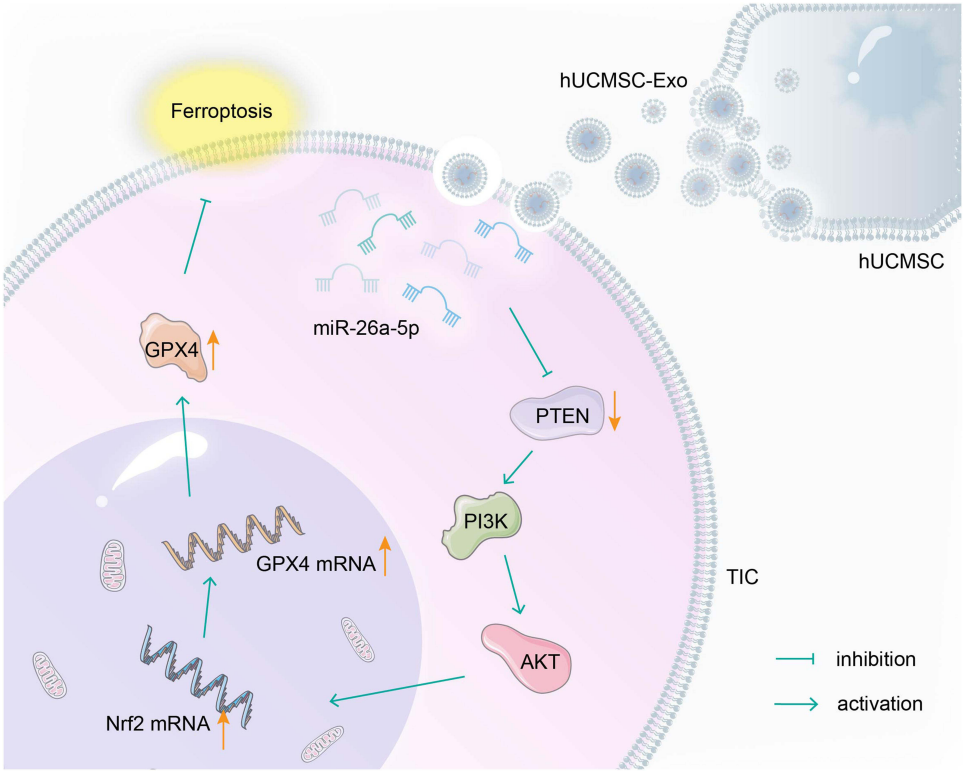

Figure 9 Schematic illustration of the protective effects of hUCMSC-Exo on TICs during POI. hUCMSCs deliver miR-26a-5p inhibits PTEN activation of the PI3K-AKT pathway, upregulates the expression of Nrf2 and GPX4 molecules, thereby inhibiting ferroptosis.

https://doi.org/10.2147/IJN.S532207

longitudinal studies are needed to fully elucidate the therapeutic implications and temporal patterns of exosomal action. Future research should address these gaps to enhance translational potential. These results suggest that hUCMSC-Exos transfers miR-26a-5p to regulate the ferroptosis of TICs via targeting the PTEN/GPX4 pathway.

Conclusion

In conclusion, the findings of this work show that hUCMSC-Exo intervention reduces the morphological and functional defects of the ovaries caused by POI. Its possible molecular mechanism involves the delivery of miR-26a-5p to target the PTEN/GPX4 axis, thereby inhibiting the TICs ferroptosis process (as shown in Figure 9). Our research highlights the potential clinical relevance of exosome miRNA in the restoration of ovarian function but also holds particular promise for stem cell-based therapeutic strategies targeting POI. Future investigations focus on translating these findings to human models or organoids, and validating the miR-26a-5p/PTEN/GPX4 pathway as a therapeutic target for primary ovarian insufficiency.

Acknowledgments

The authors declare that they have not used AI-generated work in this manuscript.

Author Contributions

All authors made a significant contribution to the work reported, whether that is in the conception, study design, execution, acquisition of data, analysis and interpretation, or in all these areas; took part in drafting, revising or critically reviewing the article; gave final approval of the version to be published; have agreed on the journal to which the article has been submitted; and agree to be accountable for all aspects of the work.

Ethics Declarations

This study followed the guidelines of "Laboratory Animal Environment and Facilities" (GB 14925-2010) and ARRIVE 2.0, and has been approved by the Ethics Committee of Binzhou Medical University: Project title: Study on the mechanism of stem cell exosomes in treating premature ovarian failure. Approval number: No. 2023-24. Date of approval: June 23, 2023.

Funding

This investigation was supported by the National Natural Science Foundation of China (No. 32200731); Natural Science Foundation of Shandong Province (No. ZR2021MC064 and ZR2021QH149); Shandong Province Higher Education Institutions "Youth Creative Team Program" Project (No. 2022KJ092).

Disclosure

The authors declared that they have no conflicts of interest in this work.

References

1. Jiao X, Ke H, Qin Y, Chen ZJ. Molecular genetics of premature ovarian insufficiency. *Trends Endocrin Met*. 2018;29(11):795–807.
2. Bao R, Xu P, Wang Y, et al. Bone marrow derived mesenchymal stem cells transplantation rescues premature ovarian insufficiency induced by chemotherapy. *Gynecol Endocrinol*. 2018;34(4):320–326. doi:10.1080/09513590.2017.1393661
3. Wang Z, Wang Y, Yang T, Li J, Yang X. Study of the reparative effects of menstrual-derived stem cells on premature ovarian failure in mice. *Stem Cell Res Ther*. 2017;8(1):11. doi:10.1186/s13287-016-0458-1
4. Ding C, Zou Q, Wang F, et al. Human amniotic mesenchymal stem cells improve ovarian function in natural aging through secreting hepatocyte growth factor and epidermal growth factor. *Stem Cell Res Ther*. 2018;9(1):55. doi:10.1186/s13287-018-0781-9
5. Dai W, Xu B, Ding L, et al. Human umbilical cord mesenchymal stem cells alleviate chemotherapy-induced premature ovarian insufficiency mouse model by suppressing ferritinophagy-mediated ferroptosis in granulosa cells. *Free Radical Bio Med*. 2024;220:1–14. doi:10.1016/j.freeradbiomed.2024.04.229
6. Torrealday S, Kodaman P, Pal L. Premature ovarian insufficiency - an update on recent advances in understanding and management. *F1000Res*. 2017;6:2069. doi:10.12688/f1000research.11948.1
7. Iqubal A, Iqubal MK, Sharma S, et al. Molecular mechanism involved in cyclophosphamide-induced cardiotoxicity: old drug with a new vision. *Life Sci*. 2019;218:112–131. doi:10.1016/j.lfs.2018.12.018
8. Zhu X, Li W, Lu M, et al. M(6)A demethylase FTO-stabilized exosomal circBRCA1 alleviates oxidative stress-induced granulosa cell damage via the miR-642a-5p/FOXO1 axis. *J Nanobiotechnol*. 2024;22(1):367. doi:10.1186/s12951-024-02583-5

9. Luo C, Wei L, Qian F, et al. LncRNA HOTAIR regulates autophagy and proliferation mechanisms in premature ovarian insufficiency through the miR-148b-3p/ATG14 axis. *Cell Death Discov*. 2024;10(1):44. doi:10.1038/s41420-024-01811-z
10. Zhang C, Yu D, Mei Y, et al. Single-cell RNA sequencing of peripheral blood reveals immune cell dysfunction in premature ovarian insufficiency. *Front Endocrinol*. 2023;14:1129657. doi:10.3389/fendo.2023.1129657
11. Guahmich NL, Man L, Wang J, et al. Human theca arises from ovarian stroma and is comprised of three discrete subtypes. *Commun Biol*. 2023;6(1):7. doi:10.1038/s42003-022-04384-8
12. Liu M, Wu K, Wu Y. The emerging role of ferroptosis in female reproductive disorders. *Biomed Pharmacother*. 2023;166:115415. doi:10.1016/j.biopha.2023.115415
13. Wang F, Liu Y, Ni F, et al. BNC1 deficiency-triggered ferroptosis through the NF2-YAP pathway induces primary ovarian insufficiency. *Nat Commun*. 2022;13(1):5871. doi:10.1038/s41467-022-33323-8
14. Hu L, Hong T, He Y, et al. Chromosome segregation-1-like gene participates in ferroptosis in human ovarian granulosa cells via nucleocytoplasmic transport. *Antioxidants-Basel*. 2024;13(8):1.
15. Vlieghe H, Leonel E, Asiabi P, Amorim CA. The characterization and therapeutic applications of ovarian theca cells: an update. *Life Sci*. 2023;317:121479. doi:10.1016/j.lfs.2023.121479
16. Yu Y, Chen M, Guo Q, et al. Human umbilical cord mesenchymal stem cell exosome-derived miR-874-3p targeting RIPK1/PGAM5 attenuates kidney tubular epithelial cell damage. *Cell Mol Biol Lett*. 2023;28(1):12. doi:10.1186/s11658-023-00425-0
17. Xu C, Zhao J, Li Q, et al. Exosomes derived from three-dimensional cultured human umbilical cord mesenchymal stem cells ameliorate pulmonary fibrosis in a mouse silicosis model. *Stem Cell Res Ther*. 2020;11(1):503. doi:10.1186/s13287-020-02023-9
18. Li Z, Zhang M, Zheng J, et al. Human umbilical cord mesenchymal stem cell-derived exosomes improve ovarian function and proliferation of premature ovarian insufficiency by regulating the hippo signaling pathway. *Front Endocrinol*. 2021;12:711902. doi:10.3389/fendo.2021.711902
19. Ding C, Zhu L, Shen H, et al. Exosomal miRNA-17-5p derived from human umbilical cord mesenchymal stem cells improves ovarian function in premature ovarian insufficiency by regulating SIRT7. *Stem Cells*. 2020;38(9):1137–1148. doi:10.1002/stem.3204
20. Zhou Y, Huang J, Zeng L, et al. Human mesenchymal stem cells derived exosomes improve ovarian function in chemotherapy-induced premature ovarian insufficiency mice by inhibiting ferroptosis through Nrf2/GPX4 pathway. *J Ovarian Res*. 2024;17(1):80. doi:10.1186/s13048-024-01403-6
21. Ling L, Feng X, Wei T, et al. Human amnion-derived mesenchymal stem cell (hAD-MSC) transplantation improves ovarian function in rats with premature ovarian insufficiency (POI) at least partly through a paracrine mechanism. *Stem Cell Res Ther*. 2019;10(1):46. doi:10.1186/s13287-019-1136-x
22. Tang Y, He Y, Huo X, et al. hUMSC-derived exosomes alleviate follicular interstitial cell autophagy by let-7a-5p/AMPK/mTOR axis in POI rats. *Stem Cell Res Ther*. 2025;16(1):291. doi:10.1186/s13287-025-04396-1
23. Luo Q, Tang Y, Jiang Z, Bao H, Fu Q, Zhang H. hUCMSCs reduce theca interstitial cells apoptosis and restore ovarian function in premature ovarian insufficiency rats through regulating NR4A1-mediated mitochondrial mechanisms. *Reprod Biol Endocrin*. 2022;20(1):125. doi:10.1186/s12958-022-00992-5
24. Wang Y, Xiong Y, Zhang A, et al. Oligosaccharide attenuates aging-related liver dysfunction by activating Nrf2 antioxidant signaling. *Food Sci Nutr*. 2020;8(7):3872–3881. doi:10.1002/fsn3.1681
25. Hade MD, Suire CN, Suo Z. Mesenchymal stem cell-derived exosomes: applications in regenerative medicine. *Cells-Basel*. 2021;10(8):1.
26. Krylova SV, Feng D. The machinery of exosomes: biogenesis, release, and uptake. *Int J Mol Sci*. 2023;24(2):1337. doi:10.3390/ijms24021337
27. Pu X, Zhang L, Zhang P, et al. Human UC-MSC-derived exosomes facilitate ovarian renovation in rats with chemotherapy-induced premature ovarian insufficiency. *Front Endocrinol*. 2023;14:1205901. doi:10.3389/fendo.2023.1205901
28. Dai F, Liu H, He J, et al. Model construction and drug therapy of primary ovarian insufficiency by ultrasound-guided injection. *Stem Cell Res Ther*. 2024;15(1):49. doi:10.1186/s13287-024-03646-y
29. Meirow D, Nugent D. The effects of radiotherapy and chemotherapy on female reproduction. *Hum Reprod Update*. 2001;7(6):535–543. doi:10.1093/humupd/7.6.535
30. Lu G, Li H, Song Z, et al. Combination of bone marrow mesenchymal stem cells and moxibustion restores cyclophosphamide-induced premature ovarian insufficiency by improving mitochondrial function and regulating mitophagy. *Stem Cell Res Ther*. 2024;15(1):102. doi:10.1186/s13287-024-03709-0
31. Liu S, Wang Y, Yang H, et al. Pyrroloquinoline quinone promotes human mesenchymal stem cell-derived mitochondria to improve premature ovarian insufficiency in mice through the SIRT1/ATM/p53 pathway. *Stem Cell Res Ther*. 2024;15(1):97. doi:10.1186/s13287-024-03705-4
32. Jiang X, Stockwell BR, Conrad M. Ferroptosis: mechanisms, biology and role in disease. *Nat Rev Mol Cell Bio*. 2021;22(4):266–282. doi:10.1038/s41580-020-00324-8
33. Dixon SJ, Olzmann JA. The cell biology of ferroptosis. *Nat Rev Mol Cell Bio*. 2024;25(6):424–442. doi:10.1038/s41580-024-00703-5
34. Tan W, Dai F, Yang D, et al. MiR-93-5p promotes granulosa cell apoptosis and ferroptosis by the NF-kB signaling pathway in polycystic ovary syndrome. *Front Immunol*. 2022;13:967151.
35. Zhang X, Zheng X, Ying X, Xie W, Yin Y, Wang X. CEBPG suppresses ferroptosis through transcriptional control of SLC7A11 in ovarian cancer. *J Transl Med*. 2023;21(1):334. doi:10.1186/s12967-023-04136-0
36. Zhang S, Liu Q, Chang M, et al. Chemotherapy impairs ovarian function through excessive ROS-induced ferroptosis. *Cell Death Dis*. 2023;14(5):340. doi:10.1038/s41419-023-05859-0
37. Yang M, Lin L, Sha C, et al. Bone marrow mesenchymal stem cell-derived exosomal miR-144-5p improves rat ovarian function after chemotherapy-induced ovarian failure by targeting PTEN. *Lab Invest*. 2020;100(3):342–352. doi:10.1038/s41374-019-0321-y
38. Derry PJ, Vo ATT, Gnanansekaran A, et al. The chemical basis of intracerebral hemorrhage and cell toxicity with contributions from eryptosis and ferroptosis. *Front Cell Neurosci*. 2020;14:603043. doi:10.3389/fncel.2020.603043
39. Liang Y, Duan L, Lu J, Xia J. Engineering exosomes for targeted drug delivery. *Theranostics*. 2021;11(7):3183–3195. doi:10.7150/thno.52570
40. Lin F, Chen W, Zhou J, et al. Mesenchymal stem cells protect against ferroptosis via exosome-mediated stabilization of SLC7A11 in acute liver injury. *Cell Death Dis*. 2022;13(3):271. doi:10.1038/s41419-022-04708-w
41. Song Y, Wang B, Zhu X, et al. Human umbilical cord blood-derived MSCs exosome attenuate myocardial injury by inhibiting ferroptosis in acute myocardial infarction mice. *Cell Biol Toxicol*. 2021;37(1):51–64. doi:10.1007/s10565-020-09530-8
42. Shen H, Yao X, Li H, et al. Role of exosomes derived from miR-133b modified MSCs in an experimental rat model of intracerebral hemorrhage. *J Mol Neurosci*. 2018;64(3):421–430. doi:10.1007/s12031-018-1041-2

43. Shi B, Wang Y, Zhao R, Long X, Deng W, Wang Z. Bone marrow mesenchymal stem cell-derived exosomal miR-21 protects C-kit+ cardiac stem cells from oxidative injury through the PTEN/PI3K/Akt axis. *PLoS One*. 2018;13(2):e0191616. doi:10.1371/journal.pone.0191616
44. Li W, Si Y, Wang Y, et al. hUCMSC-derived exosomes protect against GVHD-induced endoplasmic reticulum stress in CD4(+) T cells by targeting the miR-16-5p/ATF6/CHOP axis. *Int Immunopharmacol*. 2024;135:112315. doi:10.1016/j.intimp.2024.112315